

Role of agitation in the freezing process of liquid foods using sucrose aqueous solution as a model liquid

メタデータ	言語: English 出版者: Elsevier 公開日: 2023-05-12 キーワード: Freezing process, Agitation, Supercooling degree, Ice crystal, Torque, Rheology 作成者: 増田, 勇人, 龍崎, 友弘, 伊與田, 浩志 メールアドレス: 所属: Osaka City University, Osaka Metropolitan University, Osaka City University, Osaka Metropolitan University, Osaka City University, Osaka Metropolitan University
URL	https://ocu-omu.repo.nii.ac.jp/records/2019971

Role of agitation in the freezing process of liquid foods using sucrose aqueous solution as a model liquid

Hayato Masuda, Tomohiro Ryuzaki, Hiroyuki Iyota

Citation	Journal of Food Engineering. 330; 111100
Issue Date	2022-10
Version of Record	2022-04-25
Type	Journal Article
Textversion	Author
Rights	© 2022 Elsevier Ltd. This manuscript version is made available under the CC-BY-NC-ND 4.0 License. https://creativecommons.org/licenses/by-nc-nd/4.0/ . This is the accepted manuscript version. The formal published version is available at https://doi.org/10.1016/j.jfoodeng.2022.111100 .
DOI	10.1016/j.jfoodeng.2022.111100

Self-Archiving by Author(s)
Placed on: Osaka City University

1 **Title:**

2 Role of agitation in the freezing process of liquid foods using sucrose aqueous solution
3 as a model liquid

4

5 **Authors:**

6 Hayato Masuda*, Tomohiro Ryuzaki, Hiroyuki Iyota

7

8 **Affiliation:**

9 Department of Mechanical and Physical Engineering, Osaka City University, 3-3-138
10 Sugimoto, Sumiyoshi-ku, Osaka 558-8585, Japan

11

12 **Corresponding author:**

13 * To whom corresponded should be addressed:

14 E-mail address: hayato-masuda@osaka-cu.ac.jp

15

16 **Highlights**

- 17 · The role of agitation in the freezing process was investigated.
- 18 · Samples frozen at a higher agitation speed tends to melt at a lower temperature.

- 19 · The degree of supercooling depends on the flow conditions.
- 20 · The time scale for the nucleation and growth of ice crystals was controlled by
- 21 the agitation speed.

22

23 **Keywords:** Freezing process; Agitation; Supercooling degree; Ice crystal; Torque;

24 Rheology

25

26

27

28

29

30

31

32

33

34

35

36

37 **Abstract**

38 Agitation is often encountered in various processes, such as ice cream manufacture
39 and suspension freeze-concentration of liquid food. This study investigated the effect of
40 agitation speed on the freezing process of an aqueous sucrose solution as a preliminary
41 investigation for the development of processes that include both agitation and freezing. A
42 batch-type freezer with an anchor impeller was used. Frozen samples at a higher agitation
43 speed started to melt at a lower temperature. In addition, the degree of supercooling
44 tended to increase along with the Reynolds number. In other words, it is possible to
45 control the supercooling phenomenon, which is regarded as a stochastic phenomenon,
46 based on the agitation operation. Furthermore, the time scale for the nucleation and
47 growth of ice crystals depended on the agitation speed. Thus, it was concluded that the
48 agitation operation significantly affects freezing process of sucrose aqueous solution with
49 the batch-type freezer.

50

51

52

53

54

55 **1. Introduction**

56 In many food processing operations, the flow field, including temperature and
57 concentration distributions, in the apparatus is quite complicated, because the
58 physicochemical state of food changes during processing. Rheological properties
59 typically change, which is accompanied by thermomechanical protein denaturation
60 (Shimoyamada et al., 2019) and formation of network structure such as starch
61 gelatinization (Matsumoto et al., 2021). These changes in rheological properties
62 considerably affect the fields (flow, temperature, and concentration). From the viewpoint
63 of food engineering, one of the most critical field changes is phase change; for example,
64 boiling, condensation, evaporation, solidification, and melting. Boiling and condensation
65 are popular heating processing and cooking processes. Therefore, a lot of studies have
66 focused on heat transfer characteristics during heating and final food quality, e.g. Alhama
67 and González Fernández (2002), Luo et al. (2015), and Zou et al. (2021). Similarly,
68 cooling operations for freezing food have been investigated by many researchers. One of
69 the most attractive areas in cooling processing is the manufacture of frozen food. The
70 effect of freezing conditions on the quality of various foods has been reported by many
71 researchers, including Olivera and Salvadori (2009), Chassagne-Berces et al. (2010),
72 Cartagena et al. (2021), and Yang et al. (2021). In addition, it is known that novel

73 energetic methods, such as ultrasound or pulse magnetic field, have been applied to the
74 freezing process to improve efficiency (Tian et al., 2020; Zhang et al., 2021). In addition,
75 new techniques have been developed to assess freezing processes. Kono et al. (2021)
76 proposed a contactless method for monitoring the food freezing process using microwave
77 resonance spectroscopy. Goñi et al. (2008) applied a genetic algorithm approach to predict
78 food freezing and thawing times.

79 However, these researches were limited to static freezing, that is, without convection.
80 Dynamic freezing with forced convection is also important in food processing. For
81 example, in ice cream manufacturing process, an ice cream mix is aggressively agitated
82 in a freezer. Masuda et al. (2020) and Sawano et al. (2021) reported that the agitation
83 speed in a batch-type freezer significantly affects the internal structure of ice cream,
84 including bubble/fat globule size distribution. Agitation during freezing is also used in
85 suspension freeze-concentration, which is known as an efficient separation method from
86 a viewpoint of heat transfer. Qin et al. (2007) and Ding et al. (2021) reported that agitation
87 by a rotor with scraper is a dominant factor for heat transfer and the ice production rate
88 during suspension freeze-concentration. Thus, although the effect of forced convection
89 on the freezing process should be investigated, little research has been conducted on this
90 topic. Arora and Howell (1973) investigated the freezing phenomenon of water in a pipe

91 flow and reported that the degree of supercooling, which significantly affects the ice
92 crystal size, clearly depends on the flow condition in the tube. Brooks et al. (2020) found
93 that the flow condition in a helical coiled heat exchanger is one of important parameters
94 for freezing process of sodium chloride aqueous solutions. A similar tendency is expected
95 for freezing using a stirred vessel. For example, Shirai et al. (1985) proposed a kinetic
96 model for ice crystallization to predict ice crystal growth. However, the effect of agitation
97 on the freezing process is not comprehensively understood because they kept the agitation
98 speed constant at 600 rpm. Therefore, the investigation of the effect of agitation on
99 freezing processing is valuable for food engineers.

100 The objective of this study is to preliminarily investigate the effect of agitation speed
101 on the freezing process from a practical viewpoint, particularly supercooling phenomenon
102 and ice crystal growth process. A commercial batch-type freezer was used in this study.
103 A sucrose aqueous solution was selected as the model liquid. The temperature and torque
104 changes with time were measured during freezing. Findings and results obtained in this
105 study will be utilized to optimize the agitation operation mainly in the manufacturing
106 process of ice cream or the suspension freeze-concentration process.

107

108

109 **2. Materials and methods**

110 2.1 Experimental apparatus

111 A batch-type freezer (ICE-100, Cuisinart) with a vessel with 0.144 m diameter and
112 0.107 m height was used, as shown in Fig.1. A shaft, a torque meter (TPS-A-05NM,
113 Kyowa Electric Co., Ltd.), and an anchor-type impeller [diameter (D): 0.140 m, height
114 (H): 80 mm, thickness: (d) 10 mm] was attached to a stirrer (EUROSTAR 200 control,
115 IKA). A K-type sheathed thermocouple with a diameter of 1 mm was attached to the
116 surface 20 mm from the bottom surface. Thus, the liquid temperature near the cooling
117 surface was measured. Because the surface state, including roughness significantly
118 affected the supercooling phenomenon, the vessel was washed thoroughly after every
119 experiment. A 400-mL sucrose aqueous solution (concentration $C = 10, 25, 50$ wt%) of 4
120 °C was added, and the liquid was cooled and agitated simultaneously. The agitation speed
121 (N) was varied from 10 to 90 rpm. The liquid height was set at 30 mm. The liquid
122 temperature and torque were recorded using a data logger (mini LOGGER GL200,
123 GRAPHTEC). The flow was recorded using a video camera during the freezing process.
124 Agitation was conducted until the torque reached the rated torque (0.50 N·m). Each
125 experiment was performed three or four times, and the average values are shown in each
126 figure.

127 2.2 Measurement of rheological properties

128 After freezing, the rheological properties of the frozen samples were measured using
129 a stress-controlled rheometer (MCR102, Anton Paar GmbH) with a parallel plate with a
130 diameter of 25 mm. The sample was taken from the freezer 30 minutes after the start of
131 cooling/agitation and immediately placed on the sample stage of the rheometer, whose
132 surface temperature was maintained at -10°C . To prevent heat transfer with the
133 environment, the plate and stage were spatially covered by the hood, into which a Peltier
134 element was mounted.

135 During the measurement, the temperature of the sample stage was increased from $-$
136 10°C to 5°C at a heating rate of $0.5^{\circ}\text{C}/\text{min}$. Simultaneously, the oscillation test was
137 performed at a constant amplitude deformation, γ , 1×10^4 , and angular frequency, ω , 10
138 1/s. It was confirmed beforehand that this measurement condition was within the linear
139 viscoelastic regime of the sample.

140

141 2.3 Conversion from temporal change in torque to that in viscosity during freezing

142 The temporal change in viscosity during freezing, which is an important factor for
143 design of agitation device, is basically related to the temporal change in agitation torque.
144 To investigate the power characteristics of the batch-freezer with the impeller, the power

145 number-Reynolds number correlation was experimentally constructed, as shown in Fig.

146 2. The power number, N_p , and Reynolds number, Re , were calculated as follows:

147
$$N_p = \frac{P}{\rho N^3 D^5} \quad (1)$$

148
$$Re = \frac{D^2 \left(\frac{N}{60}\right) \rho}{\mu} \quad (2)$$

149 , where P is the power consumption [W], ρ [kg/m³] is the fluid density, and μ [Pa·s] is the
150 fluid viscosity.

151 Aqueous glycerol solutions of various concentrations were used to construct the N_p -
152 Re correlation. The measurement of N_p under a wide Re range condition was realized
153 using glycerol solutions of various concentrations because the viscosity of glycerol
154 solutions widely varies with its concentration. It should be noted that the N_p - Re
155 correlation curve is inherent to the stirred vessel. This means that the correlation does not
156 depend on fluid viscosity and density. The N_p - Re correlation curve is useful for the
157 conversion of the change in torque with time to the change in viscosity. The procedure
158 was as follows: (i) the change in the torque with time during freezing was continuously
159 measured; (ii) the torque changes were converted to the N_p change based on Eq. (1); (iii)
160 the Re corresponding to the value of N_p was estimated from Fig. 2; (iv) the viscosity was
161 calculated from Eq. (2). This method was proposed by Metzner and Otto (1957), and its
162 concept has been approved by many researchers, such as Anne-Archard et al. (2006) and

163 Kaminoyama et al. (2011). The Metzner-Otto concept is mainly utilized for not only
164 liquid mixing but also slurry agitation (Herman et al., 2012; Edifor et al., 2021). The
165 definition of viscosity of frozen material is quite complicated. Nevertheless, the apparent
166 viscosity estimated by the Metzner-Otto concept can be regarded as the “average”
167 viscosity which is practically essential to the development of agitation equipment such as
168 the agitation blade and the motor.

169 It is well known that N_p is inversely proportional to Re in the laminar flow region and
170 approaches a constant value in the turbulent flow region. As shown in Fig. 2, the flow
171 condition in the freezer is determined as follows: laminar flow when $Re \leq 100$, transition
172 flow when $100 < Re \leq 7000$, and turbulent flow when $Re > 7000$. The N_p - Re correlation
173 equations at each flow region are as follows:

174 (Laminar flow region, $Re \leq 100$)
$$N_p = \frac{160}{Re} \quad (3)$$

175 (Transition flow region, $100 < Re \leq 7000$)
$$N_p = \frac{33}{Re^{0.61}} \quad (4)$$

176 (Turbulent flow region, $Re > 7000$)
$$N_p = \frac{3.3}{Re^{0.33}} \quad (5)$$

177 It was confirmed that, in all flow regions, N_p can be adequately estimated within a
178 $\pm 15\%$ error using Eqs. (3)–(5).

179

180

181 2. 4 Statistical analysis

182 Statistical analysis was conducted if the tendency should be compared between each
183 experimental condition. Experimental data were subjected to a one-way ANOVA test. The
184 significance level of $p \leq 0.05$ was selected for all tests.

185

186 **3. Results and discussion**

187 Figure 3 shows the change in temperature and torque with time at $C = 25$ wt% and N
188 = 30 rpm. In all conditions (N and C), the aqueous sucrose solution was frozen in the
189 supercooled state. The degree of supercooling, ΔT_d , is defined as the difference between
190 the minimum temperature in the supercooling state and the freezing temperature. It was
191 confirmed that the torque increased suddenly after the supercooling state was released.
192 Based on temperature, torque, and appearance, the freezing process can be classified into
193 three states: liquid, slurry, and mushy, as shown in Fig. 4. The final state of the frozen
194 solution was more solid than the liquid. Quantitatively understanding the changes in the
195 rheological properties of solutions during freezing is valuable for food engineers. The
196 apparent viscosity can be estimated from the power consumption associated with
197 agitation.

198 As a typical example, Figure 5 shows the change in viscosity with time during

199 freezing at $C = 25$ wt% and $N = 10, 30$ and 90 rpm. In all cases, the viscosity rapidly
200 increased after the release of supercooling. In addition, the behavior of the increase in
201 viscosity with time depended on the agitation speed. Especially, the increase at $N = 90$
202 rpm was more gentle than other two cases ($N = 10$ and 30 rpm). Higher agitation
203 suppresses that ice crystals locally grow due to the enhanced dispersion of ice nuclei
204 generated. This leads to the gentle increase in viscosity. On the other hand, in the case of
205 relatively low agitation ($N = 10$ and 30 rpm), frozen materials accumulate at the front of
206 agitation without breakdown or dispersion because of poor dispersion, as shown in Fig. 4
207 (c). Understanding the viscosity increase at various conditions (C and N) is essential for
208 developing a freezer with an agitation impeller.

209 In addition, the effect of agitation speed on the rheological properties of frozen
210 products is also an important factor from a practical viewpoint. In the case of $C = 25$ wt%,
211 Figure 6 presents the storage modulus obtained by thermo-oscillatory measurement with
212 sample heating 30 min after the start of cooling/agitation at $N = 30$ and 60 rpm. In each
213 sample, there was no clear difference in the value of storage modulus in the solid and
214 liquid states. Nevertheless, the melting temperature, at which the storage modulus at $N =$
215 60 rpm started to decrease, seemed to be lower than that at $N = 30$ rpm. Higher agitation
216 speed induced ice crystal micronization. As a result, it is inferred that a micronized ice

217 crystal with a larger specific interfacial area has a lower thermal resistance. Although the
218 ice crystal size should be measured in the future, Sawano et al. (2021) reported a similar
219 tendency, as the ice cream prepared at a higher agitation speed in a batch freezer showed
220 a larger melting rate. Because only two conditions are compared in Fig. 6, further
221 investigation at various parameters (N and C) is necessary to conclude the tendency.
222 Nevertheless, it is inferred that the agitation speed is an important factor in controlling
223 the rheological and thermal properties of frozen products.

224 The effect of flow condition on the freezing process was investigated, and Figure 7
225 shows the effect of Re on the supercooling degree (ΔT_d). The physical properties of the
226 solution measured at 4°C were used to calculate Re . The results are tabulated in Table 1,
227 and one-way ANOVA was implemented. It is noted that the representative Re should be
228 considered because Re temporally changes with the viscosity during freezing. However,
229 the measurement of physical properties below the freezing temperature are technically
230 difficult due to partial/complete freezing. Thus, the values at 4°C was selected as the
231 representative values. It is noted that significant local supercooling at the cooling surface
232 was not observed in the recorded image and movie due to the periodic scraping by the
233 impeller.

234 In the case of $C = 10$ wt%, ΔT_d seems to be independent of Re . On the contrary, when

235 $700 < Re < 10000$, ΔT_d monotonically increased with Re in the case of $C = 25$ and 50
236 wt%. Although the reason for this different tendency remains unclear, this could be
237 explained by the difference in the intermolecular interaction according to the sucrose
238 concentration because the supercooling phenomenon is basically dominated by the
239 interaction between molecules (Kang et al., 2020). With respect to the case of $C = 25$ and
240 50 wt%, transition or turbulent flow conditions promote supercooling. This result is in
241 agreement with the forced-convection system results using water in a pipe (Arora and
242 Howell, 1973). Although the simple comparison with their study is not suitable because
243 of the difference in the experimental system and working fluids, fluid flow is considered
244 to be one of the factors that contribute to the supercooling phenomenon when the solution
245 is not dilute, e.g. $C \geq 25$ wt%. One of the possibilities for supercooling promotion at
246 higher Re is that the temperature distribution in the vessel becomes uniform at a higher
247 Re . Although the temperature distribution at a relatively higher Re is not considered very
248 remarkable, the small nonuniformity would affect microscale phenomena, such as
249 supercooling. Another possibility is that the unsteady disturbance in the velocity
250 component of the transition/turbulent flow has a positive effect for keeping the
251 supercooling state. To keep the supercooled liquid state, water molecules should behave
252 as liquid without phase change to solid. Higher kinetic energy input to the solution under

253 higher Re may help molecules actively motion keeping liquid state even under the
254 thermodynamically unstable condition. This microscopic assumption would be revealed
255 by molecular dynamics (MD) simulations. Kawasaki and Kim (2017) pointed out that the
256 viscosity relates to the supercooling phenomenon using MD simulations. Actually, the
257 viscosity of sucrose aqueous solution at 4°C is 0.0019 Pa·s ($C = 10$ wt%), 0.0038 Pa·s (C
258 = 25 wt%), and 0.0286 Pa·s ($C = 50$ wt%). In the future, MD simulations would also help
259 to clarify the effect of sucrose concentration on the supercooling phenomenon. Although
260 the supercooling phenomenon is somewhat stochastic (Shirai et al., 1986), control of the
261 supercooling degree, which is a driving force for ice crystal growth, is a challenging topic.
262 For example, Matsumoto et al. (2018) attempted to actively control the degree of
263 supercooling by adding surfactants. As discussed above, flow condition is one of the
264 parameters that contribute to the supercooling phenomenon. Further investigation is
265 necessary to clarify effect of flow conditions in the future.

266 Figure 8 shows a snapshot of the state immediately after the release of supercooling
267 at $C = 25$ wt% and $N =$ (a) 10, (b) 30, (c) 60, and (d) 90 rpm, i.e. $Re =$ (a) 860, (b) 2579,
268 (c) 5158, and (d) 7737. In addition, ΔT_d was (a) 1.7, (b) 4.0, (c) 5.6, and (d) 8.0°C. As
269 clearly shown in Fig. 8, a higher ΔT_d leads to a larger amount of the frozen phase. It is
270 assumed that the amount of frozen phase, that is, the product of the ice crystal, is related

271 to the sudden increase in torque after the release of supercooling, G_{Max} , which is observed
272 around 420 s in Fig. 3. To assess the kinetics of ice crystal growth, the time scale was
273 estimated from the change in torque with time. Figure 9 (a) shows the change in
274 temperature and torque with time near the release of supercooling in the case of $C = 25$
275 wt% and $N = 30$ rpm. In this case, the degree of supercooling was 5.1°C . The discrepancy
276 of ΔT_d from Fig. 8 (c) at the same experimental condition ($C = 25$ wt% and $N = 30$ rpm)
277 is simply explained by the reproducibility of supercooling phenomenon. The ice nuclei
278 were first observed around the supercooling temperature at t_a , as shown by the circles in
279 Fig. 9 (b). After that, when the torque reached G_{Max} , the ice crystals appeared to grow
280 sufficiently at t_b (Fig. 9 (c)). Thus, the time between t_a and t_b is regarded as the time scale
281 for ice crystal nucleation and growth, t_i . It is noted that the temporal decrease in torque
282 after the peak is due to the dispersion of ice crystals caused by agitation.

283 Figure 10 shows the effect of agitation speed on the time scale (t_i) at various C values.
284 The results are tabulated in Table 2, and one-way ANOVA was implemented. It was found
285 that the higher the concentration, the longer the time scale for ice crystal nucleation and
286 growth. In addition, in all cases of C , t_i monotonically decreased with an increase in
287 agitation speed. To generalize the kinetics of ice crystal growth in Fig. 10, the results are
288 converted to the non-dimensional form as the effect of non-dimensional time, $t_i^* [=$

289 $t_i \cdot (N/60)$], on Re , as shown in Fig. 11. t_i^* means the required number of impeller rotation
290 for ice crystal nucleation and growth. Figure 11 shows that, in the case of $C = 25$ and 50
291 wt%, the non-dimensional time scale for ice crystal nucleation and growth increased with
292 Re up to a certain Re which depends on the sucrose concentration (C), and then decreased.
293 This result indicates that ice crystal nucleation and growth is significantly promoted
294 above the certain Re . On the contrary, in the case of $C = 10$ wt%, the certain Re was not
295 found within experimental conditions. Thus, it was found that the dynamics of ice crystal
296 nucleation and growth depends on the sucrose concentration. Although a detailed model
297 should be constructed by distinguishing primary/secondary nucleation in the future, the
298 flow condition is considered one of the most important factors for ice crystal nucleation
299 and growth in freezing process of sucrose aqueous solution.

300

301 **4. Conclusions**

302 This study investigated the effect of agitation on the freezing process of aqueous
303 sucrose solutions at various concentrations using a batch-type freezer. From the thermo-
304 oscillatory test, it was found that the frozen sample with higher agitation speed started to
305 melt at a lower temperature. In addition, the agitation speed affected the degree of
306 supercooling. The supercooling degree increased with the Reynolds number, Re , except

307 in low concentrations of sucrose. There are two possibilities for this tendency: (i) the
308 uniform temperature distribution and (ii) velocity fluctuation at higher Re .

309 Furthermore, the time scale for the nucleation and growth of ice crystals was
310 estimated from the recorded movie and the change in torque with time. In all
311 concentration systems, the time scale decreased with agitation speed. Except in low
312 concentrations of sucrose, the non-dimensional time for ice crystal nucleation and growth
313 increased with Re up to a certain Re which depends on the sucrose concentration, and
314 then decreased. This result indicates that ice crystal nucleation and growth is significantly
315 promoted above the certain Re . Thus, agitation speed is one of the dominant factors in the
316 ice crystal growth process.

317

318 **Acknowledgements**

319 This research was partially supported by JSPS KAKENHI (grant numbers 20K21110 and
320 JP21K14450), and the Tojuro Iijima Foundation for Food Science and Technology.

321

322 **Declaration of interest**

323 The authors declare that they no conflict of interest.

324

325 **Nomenclature**

326	C	concentration [wt%]
327	D	diameter of impeller [m]
328	d	thickness of impeller [m]
329	G_{Max}	maximum torque immediately after release of supercooling [N·m]
330	H	height of impeller [m]
331	N	agitation speed [rpm]
332	N_p	power number [-]
333	P	power consumption [W]
334	Re	Reynolds number [-]
335	t_a	time at which ice nuclei were first observed [s]
336	t_b	time at which maximum torque was recorded after release of supercooling [s]
337	t_i	time scale for ice crystal nucleation and growth ($t_b - t_a$) [s]
338	<i>Greek letters</i>	
339	ΔT_d	degree of supercooling [°C]
340	γ	deformation amplitude [-]
341	μ	fluid viscosity [Pa·s]
342	ρ	fluid density [kg/m ³]

343 ω angular frequency [1/s]

344

345

346

347

348

349

350

351

352

353

354

355

356

357

358

359

360

361 **References**

- 362 Alhama, F., González Fernández, C. F., 2002. Transient thermal behaviour of phase-
363 change processes in solid foods with variable thermal properties. *J. Food Eng.* 54, 331–
364 336.
- 365 Anne-Archard, D., Marouche, M., Boisson, H. C., 2006. Hydrodynamics and Metzner–
366 Otto correlation in stirred vessels for yield stress fluids. *Chem Eng. J.* 125, 15–24.
- 367 Arora, A. P. S., Howell, J. R., 1973. An investigation of the freezing of supercooled liquid
368 in forced turbulent flow inside circular tubes. *Int. J. Heat Mass Transf.* 16, 2077–2085.
- 369 Brooks, S., Quarini, G., Tierney, M., Yun, X., Lucas, E., 2020. Conditions for continuous
370 ice slurry generation in a nylon helical coiled heat exchanger. *Therm. Sci. Eng. Prog.* 15,
371 100427.
- 372 Cartagena, L., Puértolas, E., Martínez de Marañón, I., 2021. Impact of different air blast
373 freezing conditions on the physicochemical quality of albacore (*Thunnus alalunga*)
374 pretreated by high pressure processing. *LWT.* 145, 111538.
- 375 Chassagne-Berces, S., Fonseca, F., Citeau, M., Marin, M., 2010. Freezing protocol effect
376 on quality properties of fruit tissue according to the fruit, the variety and the stage of
377 maturity. *LWT* 43, 1441–1449.
- 378 Ding, Z., Qin, F. G. F., Peng, K., Yuan, J., Huang, S., Jiang, R., Shao, Y., 2021. Heat and

379 mass transfer of scraped surface heat exchanger used for suspension freeze concentration.
380 J. Food Eng. 288, 110141.

381 Edifor, S. Y., Nguyen, Q. D., van Eyk, P., Biller, P., Hall, T., Lewis, D. M., 2021. Viscosity
382 variation of model compounds during hydrothermal liquefaction under subcritical
383 conditions of water. *Ind. Eng. Chem. Res.* 60, 980–989.

384 Goñi, S. M., Oddone, S., Segura, J. A., Mascheroni, R. H., Salvadori, V. O., 2008.
385 Prediction of foods freezing and thawing times: Artificial neural networks and genetic
386 algorithm approach. *J. Food Eng.* 84, 164–178.

387 Herman, C., Leyssens, T., Debaste, F., Hault, B., 2012. Detection of the II–I Etiracetam
388 solvent-mediated polymorphic transformation through the online monitoring of the
389 suspension apparent viscosity. *J. Cryst. Growth* 342, 57–64.

390 Kaminoyama, M., Nishi, K., Misumi, R., Otani, F., 2011. A method for determining the
391 representative apparent viscosity of highly viscous pseudoplastic liquids in a stirred
392 vessel by numerical simulation. *J. Chem. Eng. Japan* 44, 868–875.

393 Kang, T., You, Y., Jun, S., 2020. Supercooling preservation technology in food and
394 biological samples: a review focused on electric and magnetic field applications. *Food*
395 *Sci. Biotechnol.* 29, 303–321.

396 Kawasaki, K., Kim, K., 2017. Identifying time scales for violation/preservation of Stokes-

397 Einstein relation in supercooled water. *Sci. Adv.* 3, e1700399.

398 Kono, S., Imamura, H., Nakagawa, K., 2021. Non-destructive monitoring of food
399 freezing process by microwave resonance spectroscopy with an open-ended coaxial
400 resonator. *J. Food Eng.* 292, 110293.

401 Luo, L.-J., Guo, X.-N., Zhu, K.-X., 2015. Effect of steaming on the quality characteristics
402 of frozen cooked noodles. *LWT* 62, 1134–1140.

403 Masuda, H., Sawano, M., Ishihara, K., Shimoyamada, M., 2020. Effect of agitation speed
404 on freezing process of ice cream using a batch freezer. *J. Food Process Eng.* 43, e13369.

405 Matsumoto, K., Ueda, J., Ehara, K., Sakamoto, J., Furudate, Y., 2018. Active control of
406 supercooling degree using two surfactants of different molecular sizes. *Int. J. Refrig.* 85,
407 462–471.

408 Matsumoto, M., Masuda, H., Hubacz, R., Horie, T., Iyota, H., Shimoyamada, M., Ohmura,
409 N., 2021. Enzymatic starch hydrolysis performance of Taylor-Couette flow reactor with
410 ribbed inner cylinder. *Chem. Eng. Sci.* 231, 116270.

411 Metzner, A. B., Otto, R. E., 1957. Agitation of non-Newtonian fluids. *AIChE J.* 3, 3–10.

412 Olivera, D. F., Salvadori, V. O., 2009. Effect of freezing rate in textural and rheological
413 characteristics of frozen cooked organic pasta. *J. Food Eng.* 90, 271–276.

414 Qin, F. G. F., Premathilaka, Chen, X. D., Free, K. W., 2007. The shat torque change in a

415 laboratory scraped surface heat exchanger used for making ice slurries. *Asia-Pac. J. Chem.*
416 *Eng.* 2, 618–630.

417 Sawano, M., Masuda, H., Iyota, H., Shimooyamada, M., 2021. Melting characteristics of
418 ice cream prepared with various agitation speeds in batch freezer. *Chem. Eng. Trans.* 87,
419 337–342.

420 Shimoyamada, M., Ishiyama, A., Masuda, H., Egusa, S., Matsuno, M., 2019. Viscosity
421 changes of soymilk due to vacuum evaporation with moderate heating. *LWT* 112, 108255.

422 Shirai, Y., Nakanishi, K., Matsuno, R., Kamikubo, T., 1985. On the kinetics of ice
423 crystallization in batch crystallizers. *AIChE J.* 31, 676–682.

424 Shirai, Y., Sakai, K., Nakanishi, K., Matsuno, R., 1986. Analysis of ice crystallization in
425 continuous crystallizers based on a particle size-dependent growth rate model. *Chem. Eng.*
426 *Sci.* 41, 2241–2246.

427 Tian, Y., Zhang, P., Zhu, Z., Sun, D- W., 2020. Development of a single/dual-frequency
428 orthogonal ultrasound-assisted rapid freezing technique and its effects on quality
429 attributes of frozen potatoes. *J. Food Eng.* 286, 110112.

430 Yang, J., Zhang, B., Zhang, Y., Rasheed, M., Gu, S., Buo, B., 2021. Effect of freezing rate
431 and frozen storage on the rheological properties and protein structure of non-fermented
432 doughs. *J. Food Eng.* 293, 110377.

- 433 Zhang, L., Yang, Z., Deng, Q., 2021. Effects of pulsed magnetic field on freezing kinetics
434 and physical properties of water and cucumber tissue fluid. *J. Food Eng.* 288, 110149.
- 435 Zhu, Z., Sun, D.-W., Zhang, Z., Li, Y., Cheng, L., 2018. Effects of micro-nano bubbles
436 on the nucleation and crystal growth of sucrose and maltodextrin solutions during
437 ultrasound-assisted freezing process. *LWT* 92, 404–411.
- 438 Zou, J., Xu, M., Zou, Y., Yang, B., 2021. Chemical compositions and sensory
439 characteristics of pork rib and Silkie chicken soups prepared by various cooking
440 techniques. *Food Chem.* 345, 128755.

Hayato Masuda: Conceptualization, Methodolgy, Validation, Investigation, Data Curation, Writing –Original Draft, Writing – Reviewing&Editing, Visualization, Project administration, Funding acquisition,

Tomohiro Ryuzaki: Methodolgy, Validation, Investigation, Data Curation

Hiroyuki Iyota: Methodolgy, Formal analysis

Figure 1. Experimental apparatus: (a) overview and (b) anchor impeller.

Figure 2. N_p - Re correlation curve for the freezer with the impeller. The N_p is inversely proportional in laminar flow region. Correlation curves is classified into three types according to flow regions: $N_p = 160/Re$ (laminar flow region, $Re \leq 100$), $N_p = 33/Re^{0.61}$ (transition flow region, $100 < Re \leq 7000$), $N_p = 3.3/Re^{0.33}$ (turbulent flow region, $Re > 7000$).

Figure 3. The changes in temperature and torque with time during freezing at $C = 25$ wt% and $N = 30$ rpm.

Figure 4. Snapshots of the state at $C = 25$ wt% and $N = 30$ rpm: (a) liquid, (b) slurry, and (c) mushy.

Figure 5 The change in the viscosity with time estimated using Metzner-Otto concept at $C = 25$ wt%.

Figure 6. Storage modulus of frozen samples obtained via a thermo-oscillatory test ($\gamma = 1 \times 10^4$, and $\omega = 10$ 1/s, and $\Delta T/t = 0.5$ °C/min).

Figure 7. Effect of supercooling degree (ΔT_d) on Reynolds number (Re).

Figure 8. Representative snapshots of the state immediately after the release of supercooling at $C = 25$ wt%: (a) $N = 10$ rpm, $Re = 860$, $\Delta T_d = 1.7^\circ\text{C}$, (b) $N = 30$ rpm, $Re = 2579$, $\Delta T_d = 4.0^\circ\text{C}$, (c) $N = 30$ rpm, $Re = 5158$, $\Delta T_d = 5.6^\circ\text{C}$, and (d) $N = 90$ rpm, $Re = 7737$, $\Delta T_d = 8.0^\circ\text{C}$.

Figure 9. The change through supercooling at $C = 25$ wt% and $N = 30$ rpm: (a) the temporal change in temperature and torque, (b) the snapshot immediately before supercooling at t_a , and (c) immediately after supercooling at t_b . The circle in (b) presents the ice nuclei. In this experiment, the degree of supercooling was 5.1°C .

Figure 10. Effect of rotational speed of the impeller (N) on the time scale for ice crystal nucleation and growth (t_i).

Figure 11. Effect of Reynolds number (Re) on the non-dimensional time scale for ice crystal nucleation and growth (t_i^*).

Figure 1

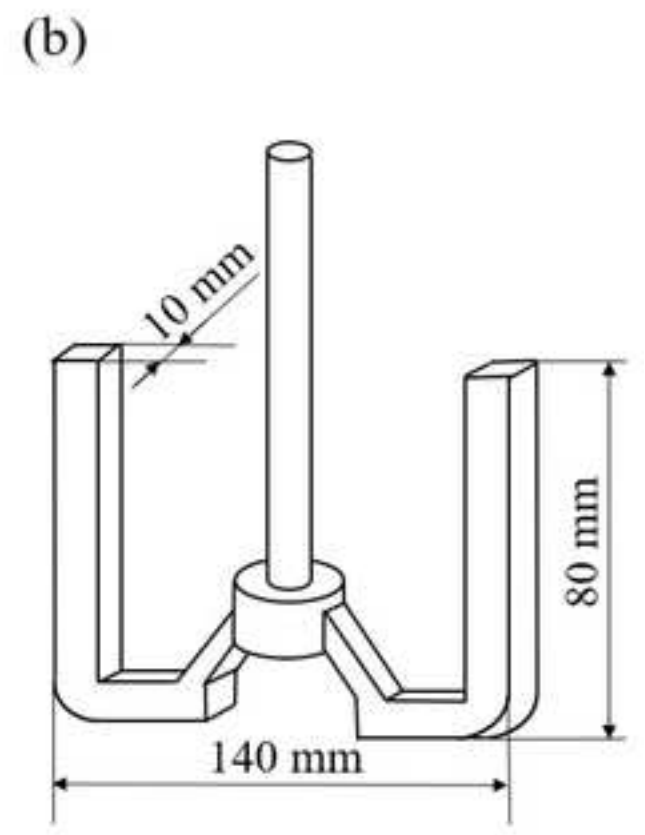
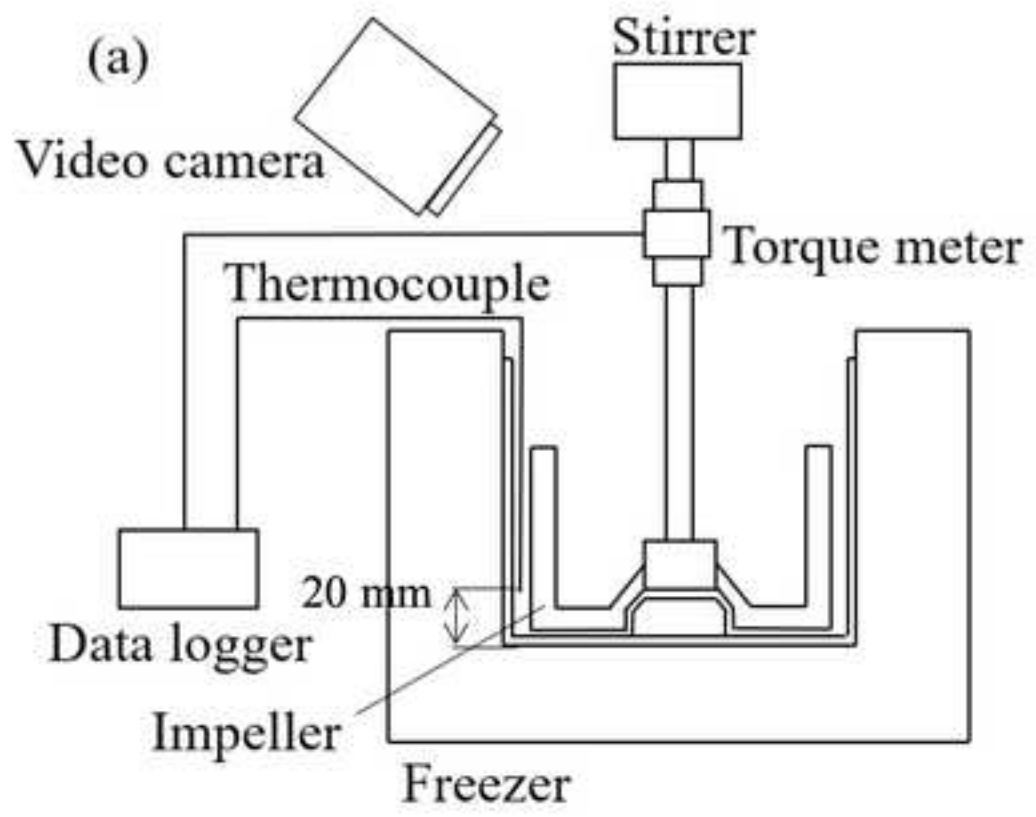


Figure 2

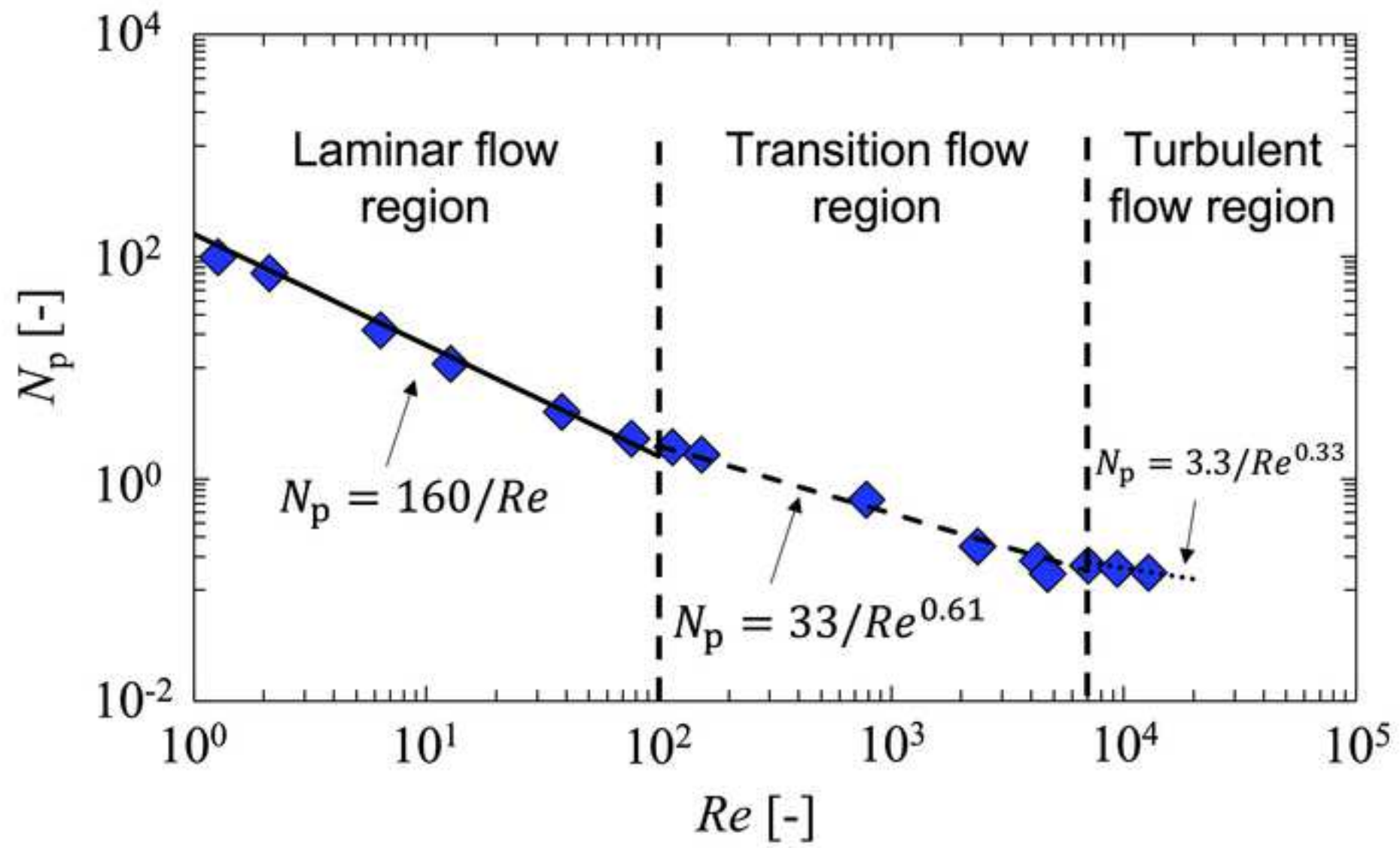


Figure 3

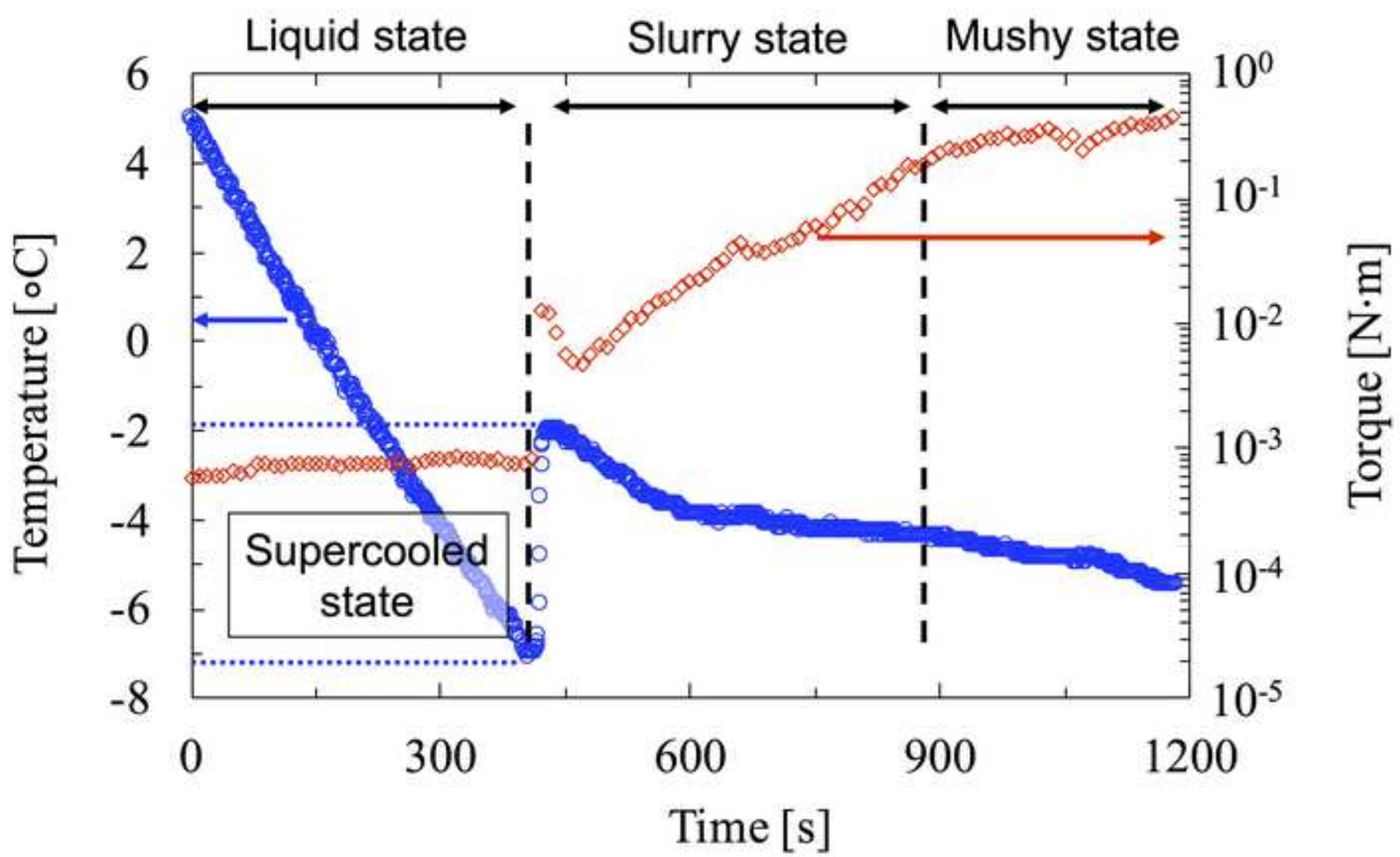


Figure 4

(a)



(b)



(c)



Figure 5

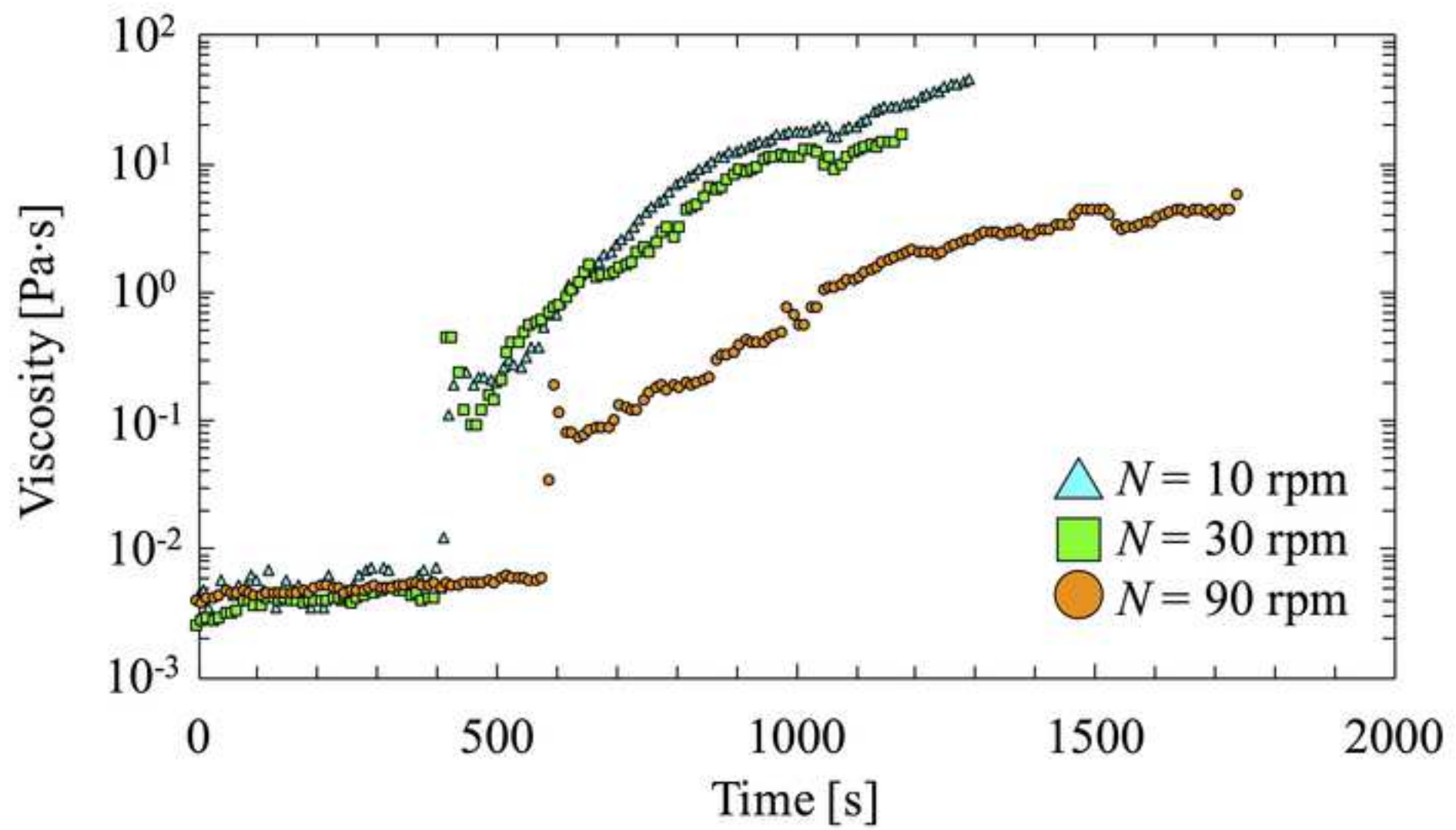


Figure 6

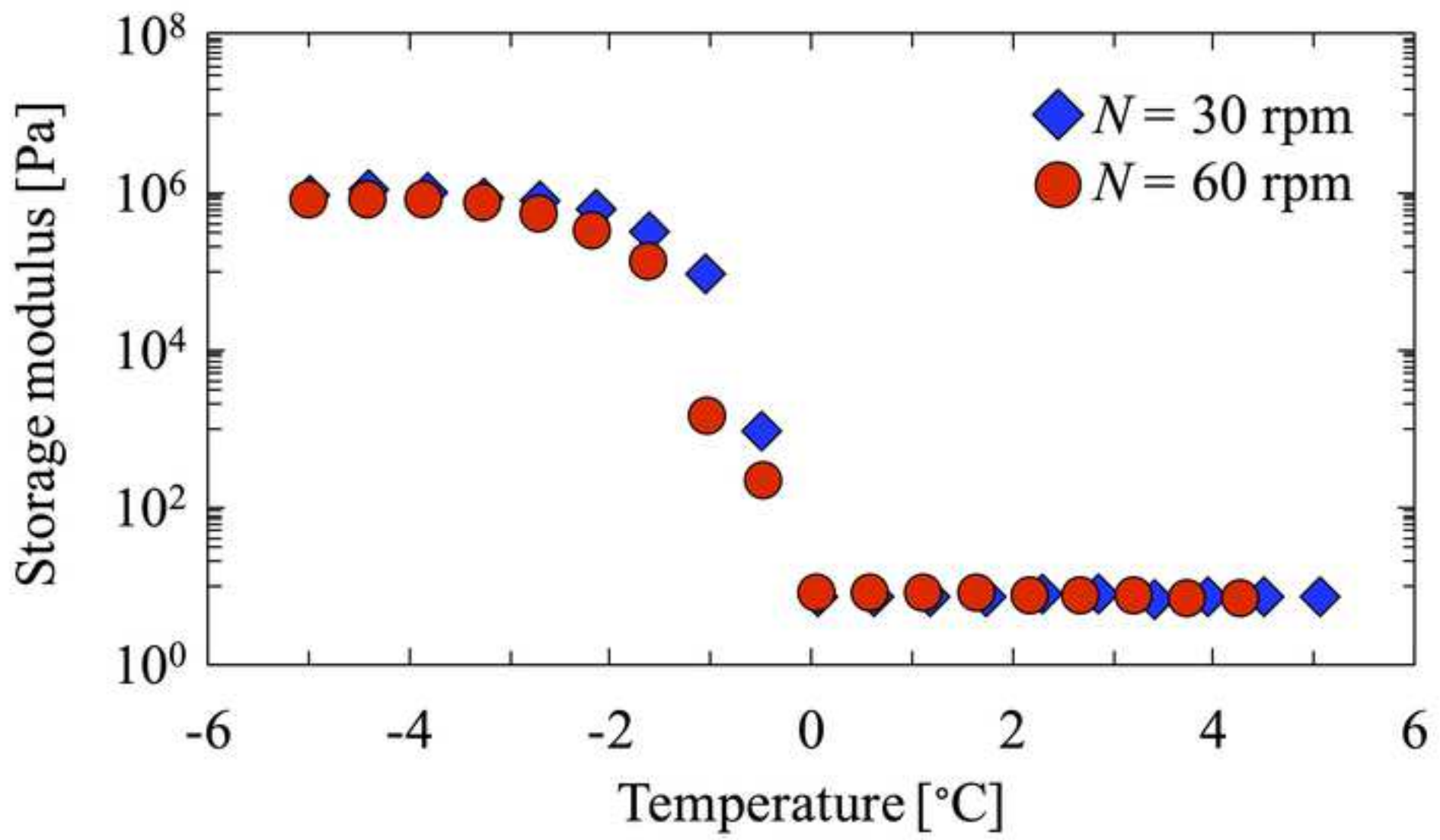


Figure 7

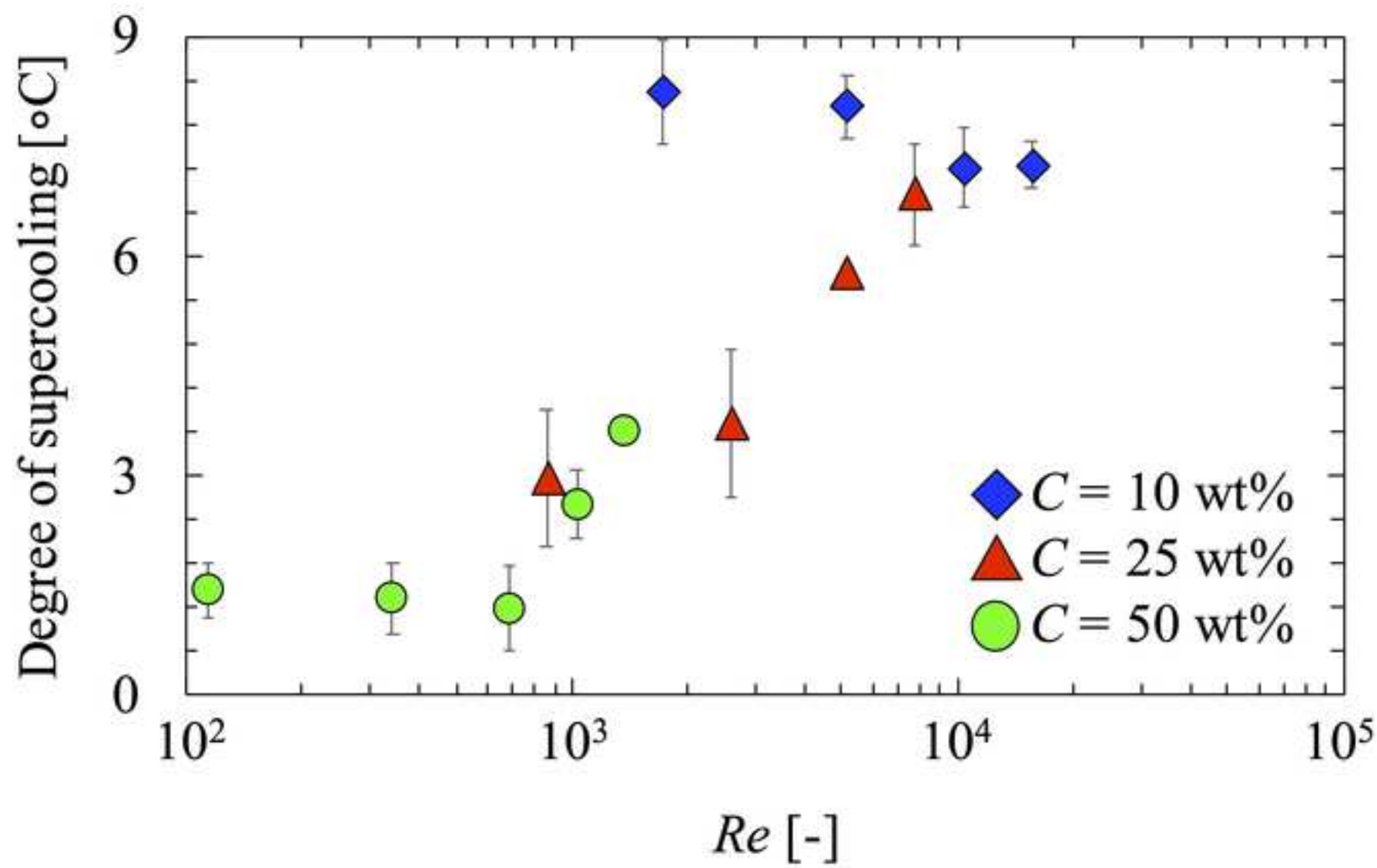
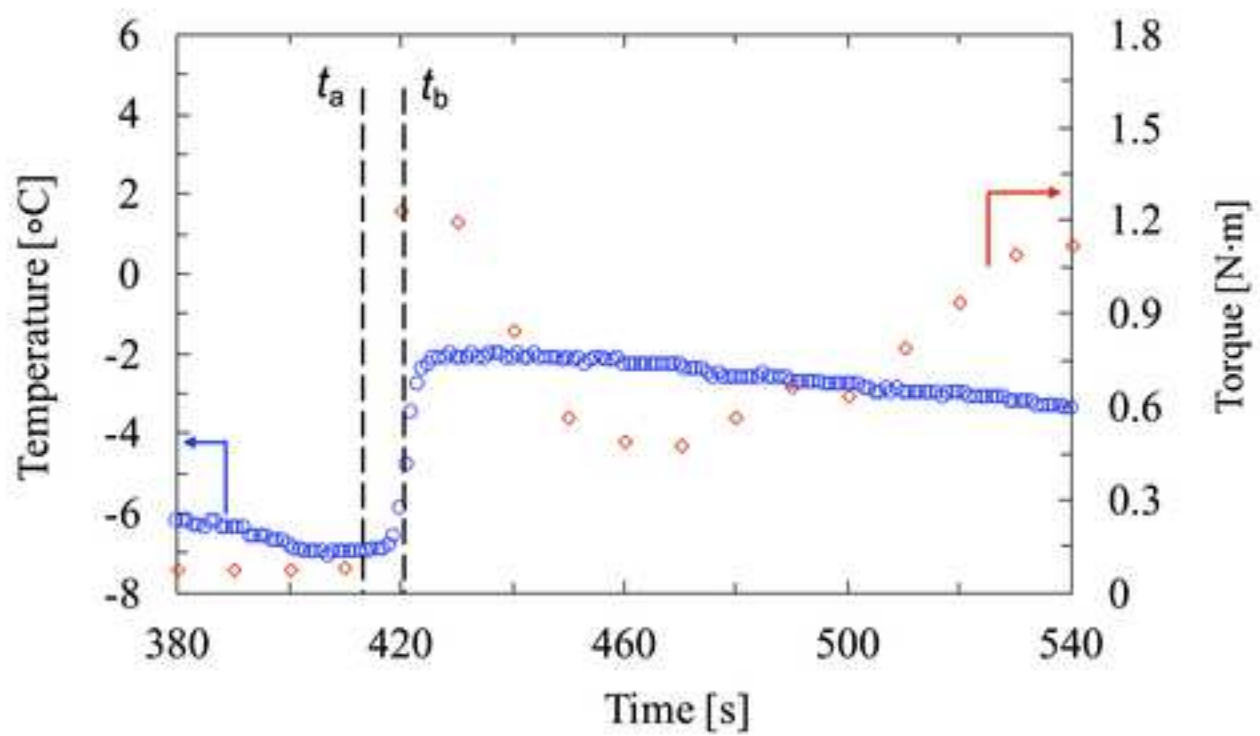


Figure 8



Figure 9

(a)



(b)



(c)



Figure 10

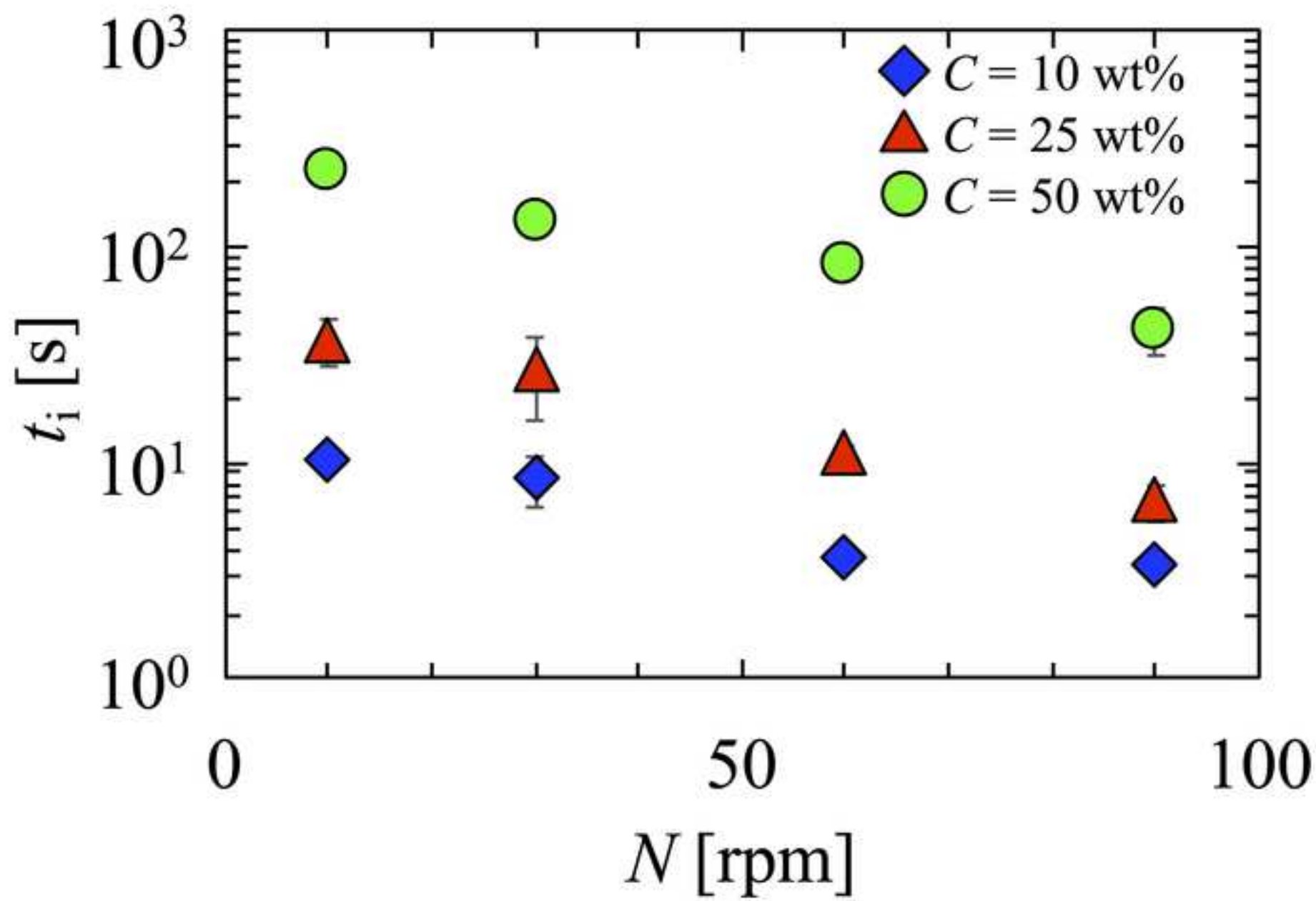


Figure 11

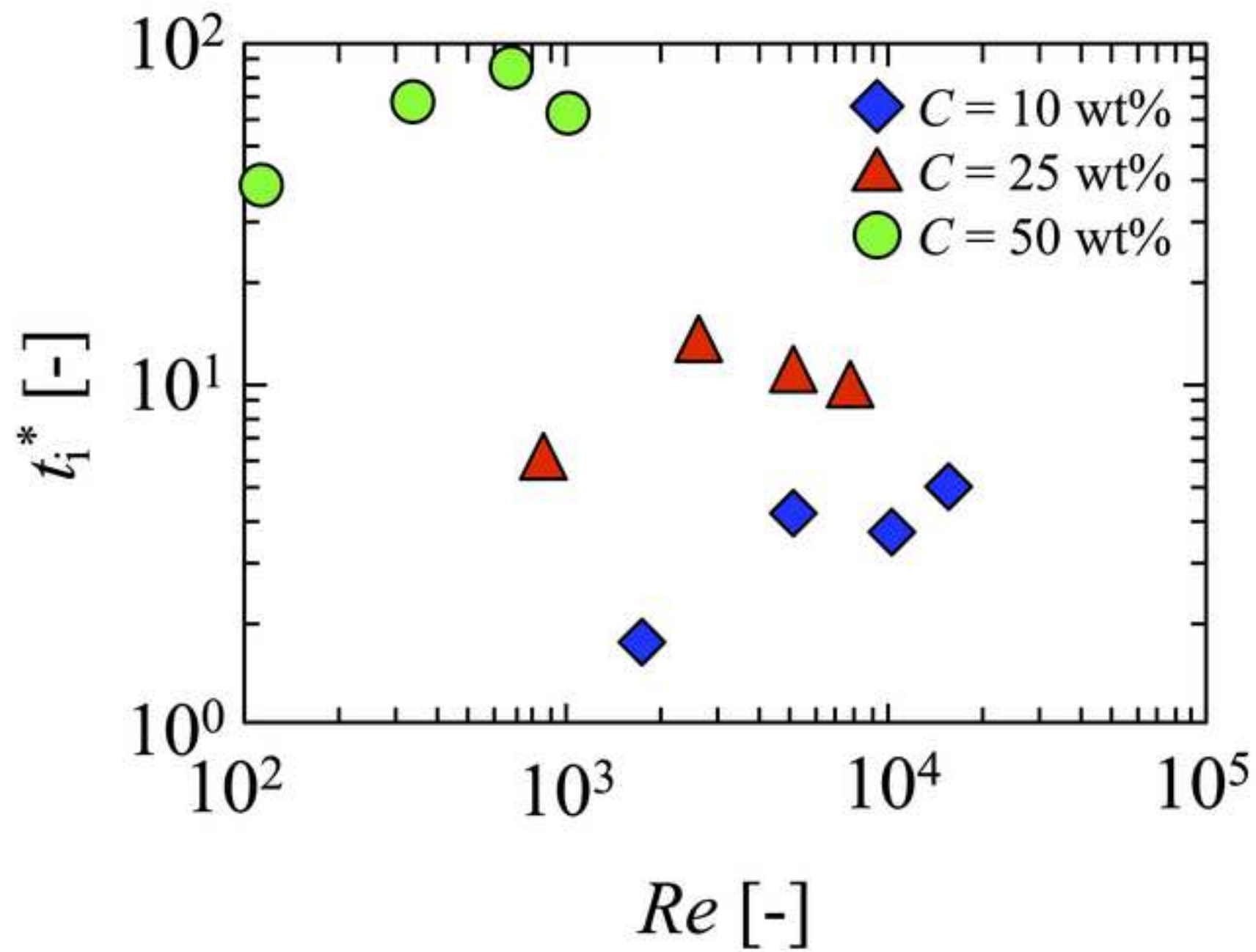


Table 1 Degree of supercooling (ΔT_d) at different experimental conditions.

N [rpm]	$C = 10$ wt%		$C = 25$ wt%		$C = 50$ wt%	
	Re [-]	ΔT_d [°C]	Re [-]	ΔT_d [°C]	Re [-]	ΔT_d [°C]
10	1719	8.23 ± 0.70^a	860	2.97 ± 0.94^b	114	1.43 ± 0.37^e
30	5158	8.03 ± 0.44^a	2579	3.7 ± 1.02^{bc}	343	1.3 ± 0.49^e
60	10316	7.20 ± 0.53^a	5158	5.77 ± 0.08^{cd}	685	1.17 ± 0.58^e
90	15474	7.23 ± 0.33^a	7737	6.83 ± 0.69^d	1028	2.6 ± 0.47^{ef}
120	–	–	–	–	1370	3.6^f

Values are mean \pm standard variation.

Values with the different superscript indicate significant difference ($p \leq 0.05$).

Table 2 Time scale for ice crystal nucleation and growth (t_i) at different experimental conditions.

N [rpm]	$C = 10$ wt%		$C = 25$ wt%		$C = 50$ wt%	
	t_i [s]	t_i [s]	t_i [s]	t_i [s]	t_i [s]	t_i [s]
10	10.33 ± 0.67^a		37.00 ± 9.02^c		227.33 ± 9.52^e	
30	8.33 ± 2.19^{ab}		27.00 ± 11.37^{cd}		133.00 ± 7.00^f	
60	3.67 ± 0.33^b		11.00 ± 1.00^d		83.33 ± 13.86^g	
90	3.33 ± 0.33^b		6.67 ± 1.33^d		41.50 ± 9.50^g	

Values are mean \pm standard variation.

Values with the different superscript indicate significant difference ($p \leq 0.05$).